DOI: 10.1002/cbic.201100747

Malachite Green Derivatives for Two-Photon RNA Detection

Jacques Lux,[a] Eduardo José Peña,[b] Frédéric Bolze,[a] Manfred Heinlein,[b] and Jean-François Nicoud*[a]

The design, preparation and characterisation of a library of malachite green (MG) derivatives for two-photon RNA labelling is described. Some of these MG derivatives exhibit an increased affinity for an MG-aptamer, as well as improved two-photon sensitivity when compared to the classical malachite green chloride. The underlying mechanisms and potential benefits for in vivo RNA visualisation are discussed.

Introduction

Although the sequencing of the genomes of many organisms, including humans, has been achieved, understanding how this stored and inherited genetic information is used to organise and maintain living cells and organisms remains a major challenge. The discovery of green fluorescent protein (GFP) in the early 1960s[1] and its subsequent application for nonintrusive imaging of cellular structures, organelles and proteins facilitated the functional analysis of genes and proteins in vivo. Increasing evidence indicates that cellular functions involve RNA molecules targeted to specific locations within cells, and that RNA processing pathways occur in association with specific subcellular structures or complexes. For example, mRNAs exit the nucleus only after they have been quality controlled, spliced, poly-adenylated and capped.[2,3] The subsequent fate of the mRNA molecules is often associated with proteins that remain bound as the RNA enters the cytoplasm.[4] Here, the RNA might be recruited by a signal-recognition particle for translation at the endoplasmic reticulum surface.[5] Other mRNAs might be transported along the cytoskeleton[6] or ER membranes,[7] and during transport, translation might be temporarily repressed to allow protein synthesis localised at final destination.[8] Also, mRNA molecules might be targeted to specific storage organelles for later use, and those destined for degradation are targeted to processing bodies (P-bodies).[9,10] In addition to mRNAs, various other classes of RNAs function in the regulation of gene expression and pathogen defence, through mechanisms commonly known as "RNA silencing".[11] These RNA molecules might act in the nucleus or cytoplasm, and might even have extracellular autonomous functions (moving between cells and tissues).[11,12] In plants, intercellular RNA transport is also common to certain RNA viruses that move their genomes between cells and systemically throughout plant tissues in a non-encapsidated form to cause systemic infection.[13] Further insights into the function of RNA molecules in relation to their associations with specific cellular structures and localisations requires imaging tools with sequence-specific detection. Unlike proteins, which can be easily imaged upon expression as translational fusions to GFP or other fluorescent adjuncts, RNA molecules require in vitro labelling and microinjection for their direct visualisation,[14] or they can be detected by indirect methods, either through hybridisation with a fluorescently tagged probe (e.g. molecular beacons),[15] or by sequence-specific binding of fluorescent proteins.[16–19] An as yet not fully explored approach is the use of aptamer-binding dyes. This RNA detection technique avoids invasive methods or the binding of bulky proteins that might interfere with RNA localisation, dynamics or function. Here, the RNA of interest is tagged with an RNA sequence selected for binding the cell-permeant dye or fluorophore through its secondary structure. The aptamer and corresponding fluorophore are created either by identification of an RNA aptamer able to bind a specific fluorophore, or by adapting a fluorophore to bind a specific RNA aptamer. The first approach has been recently applied by Paige et al. in the creation of GFP-like fluorophores.[20] By following the second approach, we here report the adaptation of malachite green (MG), a well known aptamer-binding dye.[21] To distinguish dye molecules bound to aptamer from unbound dye in vivo, it is important that aptamer binding changes the dye properties such that the aptamer-bound dye can be detected in the microscope. MG appears to be particularly suited for this purpose as aptamer binding induces a red shift in the dye absorbance and increases its fluorescence.[22] A complication of MG aptamer (MGA) labelling is the fluorescence background that results from nonspecific stabilisation of a fluorescence-emitting conformation of the dye.[23,24] In highly diffusive media and highly autofluor-

[a] Dr. J. Lux,[+] Dr. F. Bolze, Prof. Dr. J.-F. Nicoud
Laboratoire de Biophotonique et Pharmacologie, UMR 7213 UdS/CNRS
74 route du Rhin, 67401 Illkirch (France)
E-mail: jfnicoud@unistra.fr

[b] Dr. E. J. Peña,[+] Dr. M. Heinlein
Institut de Biologie Moléculaire des Plantes, CNRS UPR 2357
12, rue du Général Zimmer, 67084 Strasbourg (France)

[+] These authors contributed equally to this work.

Supporting information for this article is available on the WWW under http://dx.doi.org/10.1002/cbic.201100747.

escent samples such as plant tissues, the signal-to-noise ratio can be increased by localised excitation, for example by using two-photon excitation (TPE).[25] By restricting excitation to the focal point, the application of TPE also has the potential to reduce the phototoxic effects caused by reactive oxygen species produced by MG, other fluorophores and fluorescent proteins.[26,27] To increase the applicability of MG to in vivo imaging, we here report the design and biophysical characterisation of MG-derived triphenylmethane dyes with improved aptamer binding and two-photon (TP) brightness.

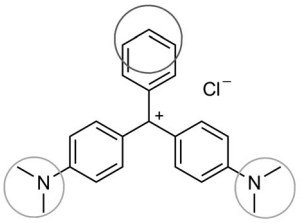

Scheme 1. Malachite Green (MG), with sites of modification highlighted.

Results and Discussion

Synthesis

MG is commercially available with various counter anions such as chloride, oxalate, or sulfate. Some of these, such as oxalate, are particularly toxic and can interfere with cellular functions. We prepared MG derivatives with chloride as the counter anion, and their properties were compared with commercially available MG chloride (MG-Cl) as reference. The structure of the MGA and its interactions with MG or with its analogue tetramethylrosamine have been studied by solid-state X-ray crystallography,[28] and in solution by NMR spectroscopy.[29,30] Binding to the aptamer induces specific conformational changes in both the RNA and the dye. The RNA folds into a pocket with the dye ligand at its centre. Specific interactions reduce the freedom of movement of individual phenyl rings of the dye, and by aligning two rings in a planar conformation, the conjugated double bonds interact and cause fluorescence upon illumination at the appropriate excitation wavelength. MG modifications have to maintain the electrostatic and base-stacking interactions with the aptamer that are required for the formation and stabilisation of the complex.[31,32] Nevertheless, as the binding process is adaptive and stabilised by an induced fit ("ligand-induced folding" or "adaptative binding"),[33–35] small modifications are possible, as they will be compensated for by corresponding small structural changes in the aptamer conformation. Several studies have investigated the structural adaptation of aptamer sequences to the corresponding dyes. As described by Brackett and Dieckmann, the phenyl ring of MG can be modified without compromising the interaction with MGA.[36] In the present work, we modified the dye by adding substituents at the *meta* and/or *para* positions of the phenyl ring. In addition, as the MG dimethylamino groups are inserted deep in the aptamer-binding pocket, we explored the effects of changing the methyl substituents at the nitrogen atoms (Scheme 1).

Modifications at the phenyl ring were mainly performed to modulate the two-photon absorption (TPA) efficiency. By introducing electroactive groups to produce a mesomeric or inductive effect (OMe, Me or I in **8a**–**d** and **12a**, **b**) we could induce a donor-conjugated system-donor architecture that is known to be efficient in TPA.[36] Furthermore, in the bound state, the modified phenyl ring adopts a more coplanar alignment with one of the other rings,[29] thus enhancing TPA by increasing π electron conjugation. We introduced the substituents at the *para* and/or *meta* positions of the phenyl ring. In order to modulate both TPA and the pharmacokinetic properties of the dye, we also tested the introduction of alkoxy and oligo(ethylene glycol) chains of various lengths (**12c**–**e**). In addition, to further increase the TPA, we extended the π system by replacement of the anisyl group of **8a**, **b** with a methoxystyryl group (**14a**, **b**). As the phenyl ring points out from the aptamer binding pocket, such long modifications were interesting to study the size "tolerance" of the adaptive binding mechanism. Modifications at the nitrogen atoms (N) included the addition of small lipophilic groups (**4a**) and of a hydroxyl group. These modifications affect interactions with phosphates in the RNA aptamer and were expected to influence aptamer binding (**4b**).

N-modified MG derivatives were prepared by reaction between benzaldehyde **1** and the desired substituted anilines **2a**, **b** in acidic conditions. The resulting *leuco*-malachite greens **3a**, **b** were then oxidised by 2,3-dichloro-5,6-dicyano-1,4-benzoquinone (DDQ) in the presence of an excess of hydrochloric acid to yield the final MG derivatives **4a** and **4b** (Scheme 2).

MG derivatives mono-substituted at the phenyl ring **8a**–**d** were prepared by reaction of Michler's ketone **5** with substituted iodo- and bromobenzenes **6a**–**d** in the presence of *n*BuLi. The resulting triphenylcarbinol derivatives **7a**–**d** were dehydrated in acidic conditions to give the corresponding MGs **8a**–**d** (Scheme 3).

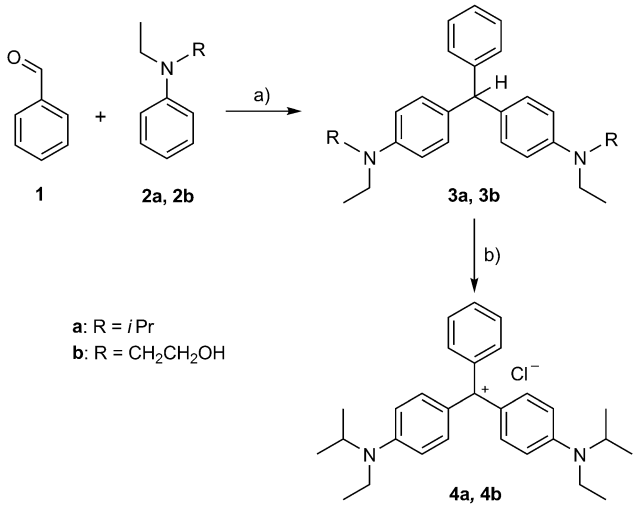

Scheme 2. Preparation of N-modified MGs **4a**, **b**. a) *p*-Toluenesulfonic acid in benzene, reflux (80 °C) with a Dean–Stark device, 48 h; b) HCl 10 M, DDQ, in benzene and MeOH, 18 h; yield: 7%.

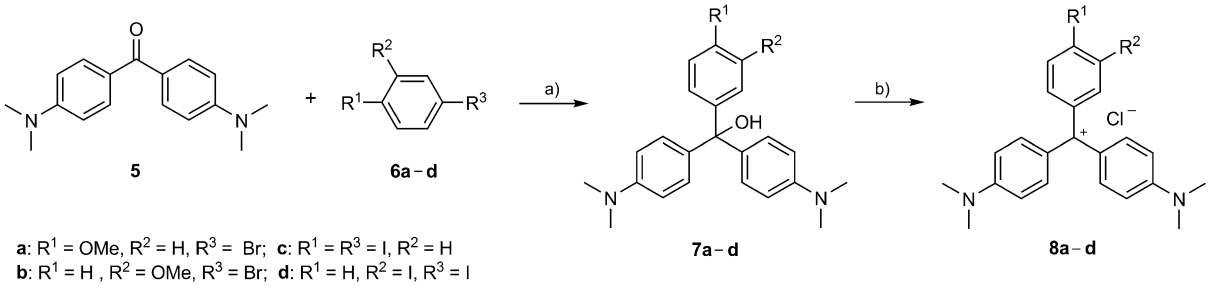

Scheme 3. Synthesis of MGs **8a–d**. a) *n*BuLi 1.6 M in THF, −78 °C, 2 h, then Michler's ketone in THF, RT, 18 h; b) HCl 10 M in CH_2Cl_2 and MeOH, 75 °C, 18 h; yield: 75–100%.

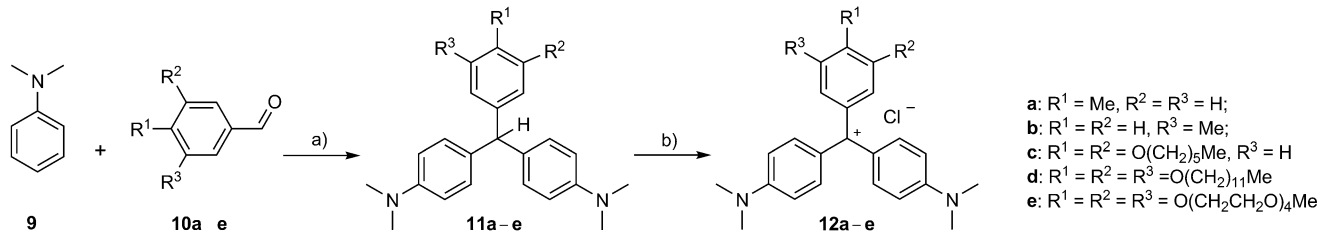

Scheme 4. Synthesis of MG **12a–e**. a) Montmorillonite K10, 100 °C, 18 h; b) HCl (10 M), DDQ or PbO_2, in CH_2Cl_2 and MeOH, RT, 18 h; yield: 5–10%.

MG derivatives **12a–e** were prepared by reaction of *N*,*N*-dimethylaniline **9** with the corresponding benzaldehydes **10a–e** in the presence of montmorillonite K10, followed by PbO_2 oxidation of the intermediary *leuco*-derivatives **11a–e** with an excess of HCl (Scheme 4).

In order to increase the length of the conjugated systems to improve the TP properties, palladium Heck cross-couplings were performed on the *para*- and *meta*-iodo derivatives **8c, d** with *para*-methoxystyrene **13** to yield MG derivatives **14a, b** (Scheme 5).

All new compounds were characterised by ^1H and ^{13}C NMR spectroscopy and high-resolution mass spectrometry. Experimental details and the results of these characterisations are provided in the Supporting Information.

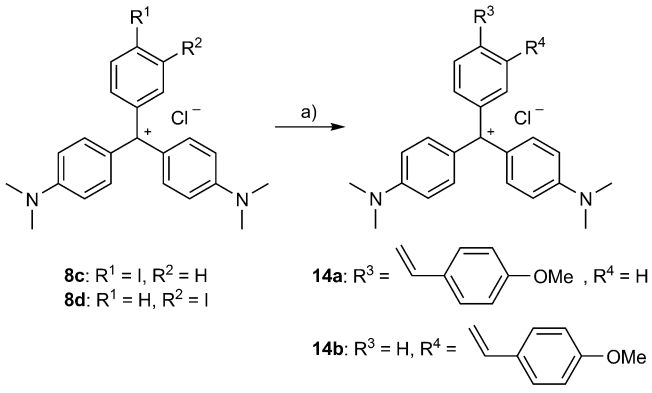

Scheme 5. Preparation of MGs **14a, b**. a) **13**, $Pd(OAc)_2$, tri-o-tolylphosphine in triethylamine and xylene (or DMF), 142 °C, 48 h, then PbO_2 and HCl (10 M) in CH_2Cl_2 and MeOH, 18 h; yield: 25%.

One-photon properties

UV–visible absorption of the MG derivatives was studied in aqueous solution. Figure 1 shows typical absorption spectra of MG derivatives **4a**, **8a** and MG-Cl.

The λ_{max}^{abs} and ε values for the new MG derivatives are listed in Table 1. Absorption values lie in the 607–632 nm range, thus indicating a weak effect of the various modifications on λ_{max}^{abs}. The most bathochromically and hypsochromically shifted absorption bands were found for the isopropyl derivative **4a** and the *m*-iodo derivative **8d**, respectively. We did not find any correlation between the substitutions on the phenyl ring and a bathochromic shift due to the increased conjugation length

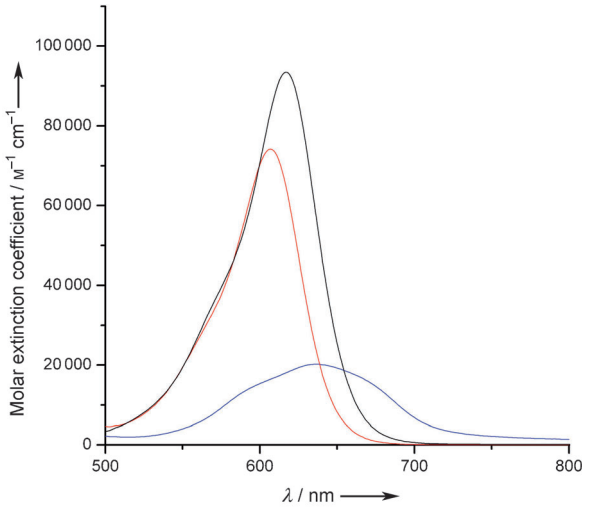

Figure 1. Selected UV/Vis spectra of MG derivatives in water. MG-Cl (black), **8a** (red) and **4a** (blue).

Table 1. UV–visible λ_{max}^{abs} and ε_{max} of new MG derivatives in HEPES buffer (pH 7.4).

Compound		λ_{max}^{abs} [nm]	ε_{max} [$M^{-1}cm^{-1}$]	Compound		λ_{max}^{abs} [nm]	ε_{max} [$M^{-1}cm^{-1}$]
4a	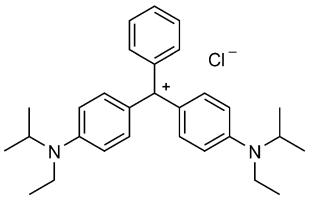	632	19900	**4b**	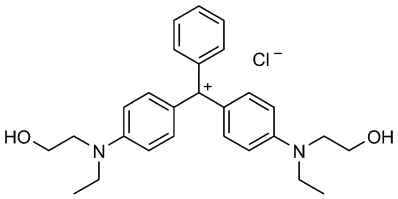	622	31100
8a	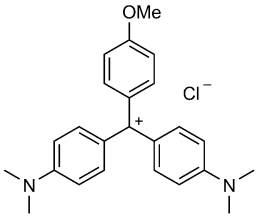	607	74100	**8b**	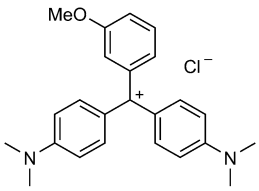	619	50500
8c	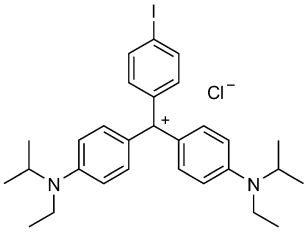	622	64900	**8d**	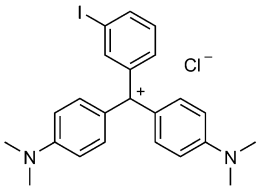	607	21100
12a	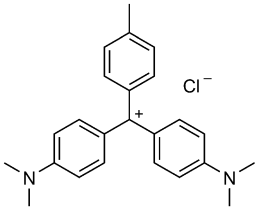	612	39600	**12b**	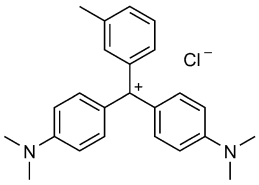	615	34300
12c	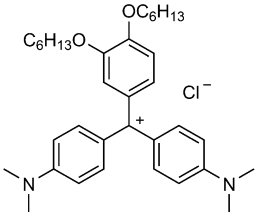	619	17000	**12d**	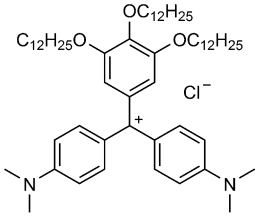	628	21200
12e	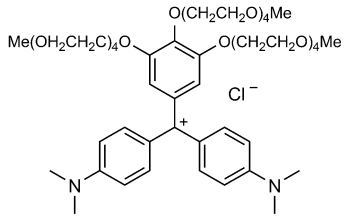	620	24000	**14a**[a]	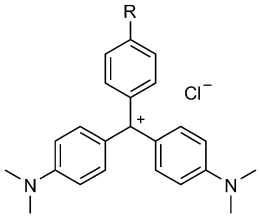	624	47900
14b[a]	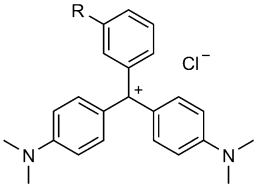	623	22300	MG-Cl	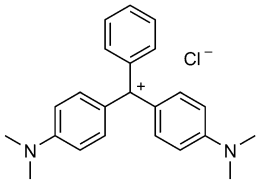	617	92400

[a] R = 4-methoxystyryl: 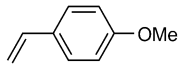

nor the presence of electron donating groups, thus indicating weak conjugation between this phenyl ring and the two dimethylaniline residues. In contrast, molar absorption coefficients are highly affected by these modifications, as described in a previous study on fluorinated derivatives of MG.[37] The unmodified MG chloride showed the highest ε_{max} (92 400 $M^{-1}cm^{-1}$), with *p*-iodo and *p*-methoxy derivatives in the same high range. A reduced absorption coefficient was observed for the *p*-methylated, *p*-methoxyvinylated, and *m*-methoxylated derivatives. The N-modified MGs showed further reduced ε_{max} values. The lowest absorption coefficients were shown by the alkoxylated MGs. Very weak fluorescence was detected for all new derivatives (quantum yields, 10^{-4}–10^{-5}), thus indicating efficient nonradiative decay in solution except for **14b,** which was slightly fluorescent (in this case, the steric hindrance of the large substituent in the *meta* position can slow the rotation of the phenyl ring, and diminish the nonradiative decay rate).

MG derivatives and MGA interaction

Consistent with previous reports, we noticed a significant red shift (15–20 nm) in the λ_{max}^{abs} for MG derivatives **8a**–**d**, **12a**–**c** and **14a** upon addition of MGA, which indicates nearly complete binding (data not shown).[21] In contrast, **4a**, **b**, **12d**, **e** and **14b** did not show any change in the λ_{max}^{abs} upon addition of aptamer, thus indicating that the specific modification in these derivatives interferes with aptamer binding. The interaction of the MG derivatives with MGA was further tested by one-photon fluorescence titration experiments in which increasing quantities of the MGA were added to a fixed 0.32 μM solution of the respective MG derivative, with fluorescence measured after each addition (Figure 2).

The dissociation constants were extracted from these titration curves by nonlinear curve fitting for a 1:1 binding, and the obtained values are shown in Table 2 (full data are available in the Supporting Information).

Under our conditions, the dissociation constant (K_d) of the reference MG-Cl was 170 nM, which is very similar to that previously published (117 nM).[22] We found that several derivatives retained an ability to bind MGA, and two of them showed increased affinity (K_d 150 nM (**8b)** and 110 nM (**12b**)). Four other MG derivatives also exhibited K_d values in the nanomolar range (**8d**, **8c**, **14a** and **12a:** 300, 320 540 and 550 nM respectively). Compounds **8a** and **12c** showed dissociation constants in the micromolar range (1.43 and 1.82 μM, respectively). For **14b**, which was already slightly fluorescent in solution, the addition of MGA resulted in only a weak increase in fluorescence. The remaining four derivatives (**4a, 4b, 12d** and **12e**) lost binding to the aptamer. The two N-modified compounds belong to this category, thus indicating that the modification at the two nitrogen atoms (located in the centre of the recognition pocket of the aptamer) impair the binding because of steric hindrance. Compounds **12d** and **12e** also lost their aptamer-binding abilities, thus indicating that the aptamer is unable to adapt its conformation to a thrice-modified phenyl ring. Interestingly, two substitutions, at *meta* and *para* positions of the phenyl ring (**12c**), preserved a moderate binding capability. Thus, one free *meta* position appears to be necessary for aptamer binding. The dissociation constants of the monosubstituted MG derivatives indicate that substitutions by a small group (I, Me, OMe) are tolerated, and aptamer binding prefers substitutions at the *meta*- over the *para*-position. Moreover, among the selected groups, adding electron-donor sub-

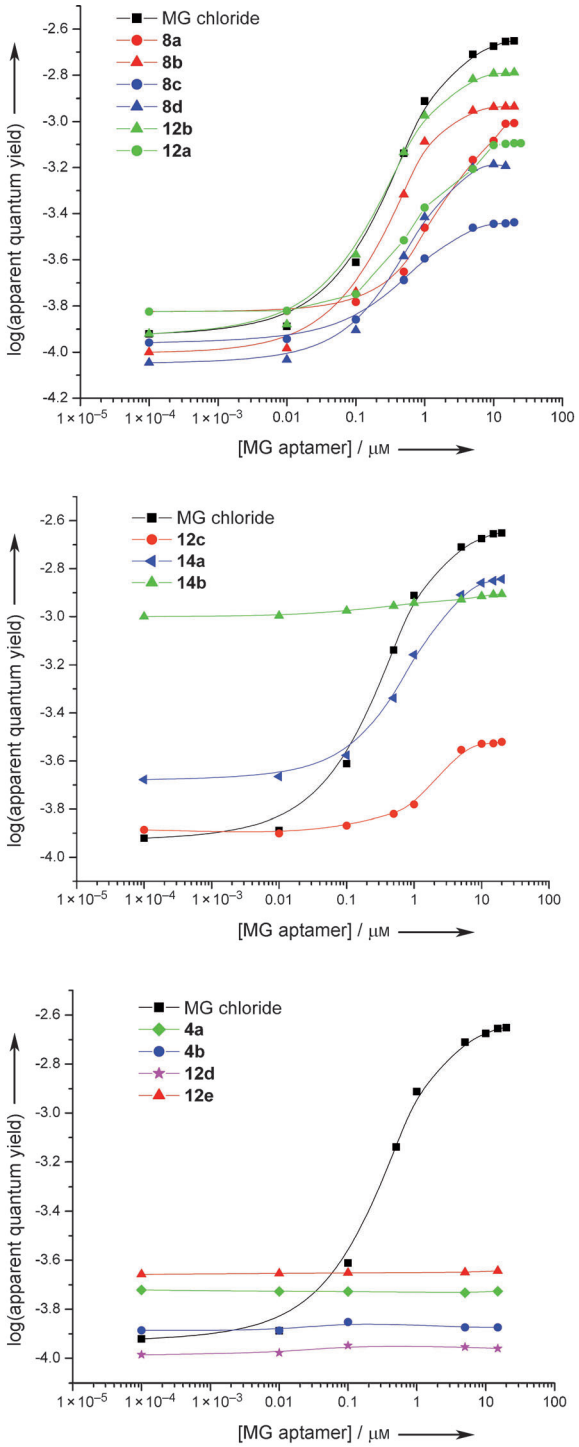

Figure 2. Apparent quantum yields for MG derivatives as function of MGA concentration.

Table 2. Dissociation constants of MGs with MG aptamer obtained by one-photon fluorescence titration; two-photon diffusion times and two-photon brightness of MG derivatives in the presence of the RNA aptamer and in the presence of a negative control RNA.

MGs	Dissociation constant [μM]	Diffusion time [ms] neg./pos.	TP brightness neg./pos.[d]
4a	n.b.[a]	–/–[b]	–/–
4b	n.b.	–/–	–/–
8a	1.43	<0.01/0.04	0.3/1.2
8b	0.15	<0.01/0.08	0.2/0.7
8c	0.32	0.02/0.05	0.1/2.1
8d	0.30	<0.01/0.02	0.2/3.9
12a	0.55	<0.01/0.02	0.3/1.7
12b	0.11	<0.01/0.08	0.5/1.6
12c	1.82	–/0.13	–/0.3
12d	n.b.	–/<0.01	–/0.4
12e	n.b.	–/–	–/–
14a	0.54	<0.01/0.023	0.6/2.7
14b	l.b.[c]	–	–
MG-Cl	0.17	0.01/0.06	0.3/0.6

[a] n.b.: no binding. [b] Very low fluorescence signal inducing low quality data for FCS measurements. [c] l.b.: low binding. [d] TP brightness of rhodamine B measured under the same conditions is 7.9.

stituents (OMe, Me) in the *para* position resulted in increased MG affinity. Interestingly, introduction of a rigid conjugated linker in a *para* position (double bond) on the free phenyl ring of MG allowed significant binding with the aptamer, even when this linker was associated with a bulky 4-vinylanisyl group (**14a**, 540 nM). In contrast, introducing the same substitution in *meta* position interfered with induced fluorescence in the presence of MGA (**14b**), as observed for the previously described small groups.

Two-photon photophysical properties

To test the TP sensitivity of the new MG derivatives we performed two-photon excited fluorescence correlation spectroscopy (TP-FCS) measurements in solutions that contained either MGA (positive control) or a modified MGA that did not bind to MG (negative control; for sequences see the Supporting Information).[21] This technique provided measurement of the relative TP brightnesses and diffusion times of the molecules (Table 2). In FCS the diffusion time is related to the size of the fluorescent moiety: a short diffusion time indicates a relatively small size of molecule (typically free MGs), whereas a longer diffusion time indicates the formation of a larger complex (i.e., MGA:MG). The low fluorescence of MG and its derivatives in the absence of aptamer was usually sufficient for extracting values for TP brightness and diffusion time. In the presence of modified MGA we obtained values close to or below 0.01 ms for all MGs, thus indicating a small diffusing molecule with low TP brightness, as expected. This clearly indicated that no binding occurred between the modified RNA aptamer and the dyes. As expected, based on the one-photon experiments, we observed an increase in TP brightness in the presence of the functional MGA. The reference MG-Cl showed a twofold increase in TP brightness upon recognition of the aptamer (Table 2). This increase in TP brightness was stronger for all MG derivatives modified at the phenyl ring. The best values were obtained with **8c** and **8d** (21- and 19.5-fold increase in TP brightness, respectively). For the MG derivatives with the highest affinity for MGA (**8b** and **12b)**, the increase in TP brightness was 3–3.5-fold. Thus, these derivatives are superior to MG-Cl in terms of both aptamer binding and TP brightness. The relative TP brightness can be correlated with the electronic effects of the specific substituents. Relative to MG-Cl, the introduction of an electroactive group (donor or acceptor) improved TP brightness. The increase in TP brightness was more pronounced with the more efficient acceptor groups (in our case iodide, with Hammett constants of +0.28 and +0.34 for the *para* (**8c**) and *meta* (**8d**) substitutions, respectively). The *meta*-substituted iodo compound **8d** appeared to be more efficient than the *para* compound **8c**, likely attributable to the distance dependence of the inductive effect. The *meta*-OMe substitution resulted in a TP brightness similar to that of MG, mainly because of its mesomeric effect (low for the nonconjugated *meta* position; Hammett constant +0.1 for **8b**). The *para*-OMe substitution provided a strong electron-donating effect in a conjugated position (Hammett constant −0.28 for **8a**), and thus a doubled TP brightness compared to MG. The Me substitution induces an interesting increase of the TP brightness, which is more pronounced in the *meta* than in the *para* position, as would be expected for a dominant inductive effect (Hammett constants of −0.14 and −0.28 for *para* and *meta* substitution **12a** and **12b**, respectively).

Compared with the one-photon properties of RNA mimics of GFP described by Paige et al.,[20] our MG derivatives exhibit reduced one-photon brightnesses compared to that of their RNA–fluorophore complex ("Spinach"). However, in contrast to Spinach, our dyes were optimised for TP illumination. For example, the TP brightness of **8d**–MGA was about ten times higher than that of GFP (see the Supporting Information).

As MG-Cl acts as sensitizer in one-photon chromophore-assisted light inactivation (CALI),[26] that is, the degradation of the MG-bound molecule,[21] it was important to demonstrate that TPE imaging conditions do not trigger CALI and degradation of the bound aptamer. Therefore, a solution of MGA:MG-Cl was irradiated under a TP microscope (Supporting Information). The RNA was then analysed by acrylamide gel electrophoresis. No degradation was detected, thus indicating that no CALI occurred under these illumination conditions (Figure S15 in the Supporting Information). The same results were obtained when using one photon microscopy with a 633 nm laser and a Zeiss LSM510 confocal microscope (data not shown).

Cell toxicity

Cytotoxic and genotoxic effects have been attributed to MG in fungi and bacteria,[38–40] whereas MG tolerance has been associated with detoxification systems linked to respiratory processes and maintenance of the redox balance that protect cells from oxidative damage.[41,42] During this work, cell toxicity of MG and the MG derivatives was tested by measuring their effects

on the propagation of cultured tobacco Bright Yellow 2 (BY-2) cells in suspension.[43] As was reported previously for yeast, worms and flies,[21] MG freely diffused into BY-2 cells (data not shown), and the cells could tolerate MG in the culture medium; that is, they grew normally in the presence of 1.0 μM MG-Cl (Figure S16). The MG derivatives synthesised during this work showed a broad spectrum of toxicity. Specific derivatives (**14a**, **8d**, **8c** and **12a**) affected growth (even at 1.0 μM), which reflects a toxicity similar to that of MG-oxalate. Two derivatives (**12a** and **8b**) showed toxicity levels similar to that of MG-Cl. Three derivatives showed slightly reduced toxicity (**12b**, **4a** and **12c**) and the last group (derivatives **4b**, **12d**, **12e** and **14b**), did not show any toxic effect on BY-2 cells at the assayed concentrations. These derivatives did not bind to MGA or show high K_d values (Figure 3 and Table 2), thus indicating that properties affecting MGA association are involved in MG toxicity in plant cells. Interestingly, **14a** and **14b** differ only with respect to the position of the 4-vinylanisole moiety at the phenyl ring, but they are derivatives with very different toxicities. Thus, the presence of this group at the *para* position (**14a**) allowed MG to bind MGA but also resulted in its strong toxicity. In contrast, this group in the *meta* position (**14b**) interfered with MGA binding and abolished the toxic effect of the molecule. However, changes in MGA binding affinity do not necessarily correlate with changes in toxicity. Thus, although the mono-methylated derivatives **12a** and **12b** differed in MGA binding affinity they showed similar levels of toxicity.

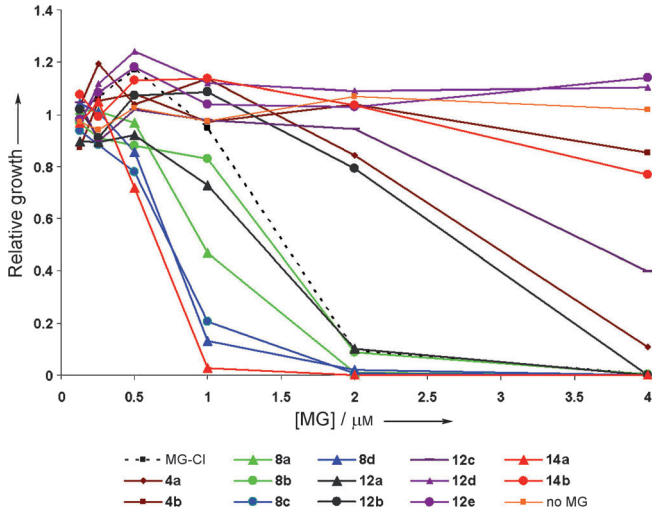

Figure 3. Relative BY-2 cell density six days after addition of MG-Cl or MG derivatives at the given concentrations.

Conclusion

A library of MG derivatives for TP detection of MGA-tagged RNAs was designed, synthesised and characterised. In particular, their TP photophysical properties have been investigated for the first time. Modifications performed at the nitrogen atoms induced a loss of MGA binding, whereas binding was preserved upon introduction of modifications at the phenyl ring. Substitutions at the *meta* position of the phenyl ring (introducing small electron-donor groups) improved the affinity for MGA. The introduction of electroactive groups at the *meta* or *para* position of the phenyl ring significantly improved the two-photon brightness of such molecules upon MGA recognition. Properties affecting MGA binding are involved in MG toxicity in plant cells. *meta*- and *para*-iodo derivatives (**8c**, **d**) showed the best signal-to-noise ratio, with TP brightnesses up to ten times higher than that of GFP for **8d**. As these derivatives also exhibited strong MGA binding, they might be recommended for in vivo visualisation of MGA-tagged RNA molecules by TPE microscopy. Moreover, the MG aptamer is significantly shorter (38 nt) than the Spinach aptamer (80 nt), which might be a critical factor in in vivo RNA labelling.

Experimental Section

Synthesis: All chemicals and reagents were purchased from Sigma–Aldrich or Acros Organics and were used as received unless specified. THF was distilled over sodium and benzophenone under argon atmosphere; dichloromethane was distilled over calcium hydride under argon atmosphere; triethylamine was distilled over potassium hydroxide under argon atmosphere; DMSO was distilled over calcium hydride under vacuum and conditioned under argon prior to use. ^{1}H and ^{13}C NMR spectra were recorded with a 400 MHz Advance 400 instrument (Bruker) in $CDCl_3$ (internal standard 7.24 ppm for ^{1}H, and 77 ppm, middle of the three peaks, for ^{13}C spectra) or [D_6]DMSO (internal standard 2.26 ppm, 39.5 ppm for ^{13}C spectra). Fast atomic bombardment (FAB) mass spectra were recorded with a ZA-HF instrument with 4-nitrobenzyl alcohol as a matrix, and ESI spectra were obtained on a Bruker HTC ultra (ESI-IT). TLC analyses were run on precoated aluminium plates (Si 60 F254; Merck). Column chromatography was run on Silica Gel (60–120 mesh; Merck). MGAs were purchased from IBA (Göttingen, Germany); for sequences see the Supporting Information.

One-photon photophysics: UV–visible spectra were recorded on a Carry 4000 spectrophotometer (Agilent Technologies, Santa Clara, CA) with paired 1 cm optical path quartz cuvettes and HEPES buffer in the reference cuvette. Fluorescence spectra were recorded on a Fluorolog spectrofluorimeter (Jobin–Yvon/HORIBA Scientific, Edison, NJ), in 1×0.4 cm fluorescence quartz cuvettes. Quantum yields were calculated with cresyl violet as the reference. Fluorescence titration curves were obtained by addition of increasing concentrations of MGA and computed as described by Babendure et al.[8] with Origin software (see the Supporting Information).

Two-photon fluorescence correlation spectroscopy: TP FCS was performed on a home-built setup. TPE was provided by a Tsunami Ti:sapphire laser pumped with a Millennia V solid-state laser (Spectra-Physics, Mountain View, CA) with 100 fs pulses (80 MHz, 760 nm). Following passage through a beam expander, the infrared light was focused into the sample by a water-immersion Olympus objective (60×, NA = 1.2) mounted on an Olympus IX70 inverted microscope. The back aperture of the objective was slightly overfilled to create a diffraction-limited focal spot. Samples were placed in eight wells of a Lab-Tek chambered cover glass (Nalge Nunc International, Rochester, NY) and positioned in the X and Y axes by a motorised stage (Märzhäuser Wetzlar, Germany). The fluorescence from the samples was collected through the same objective and directed by a COWL750 dichroic mirror (Coherent,

Orsay, France) toward a 50 μm diameter optical fibre coupled to a SPCM 200 FC avalanche photodiode (EG&G, Vaudreuil, Canada). Residual infrared light was rejected by a BG39 filter (Coherent). For FCS measurements, the normalised autocorrelation function (ACF), $G(\tau)$, of the fluorescence intensity fluctuations was calculated online by an ALV5000E digital correlator card (ALV, Langen, Germany). Calibration of the system was performed with 50 nM tetramethylrhodamine (TMR). By assuming a diffusion constant of 2.8×10^{-10} $m^2 s^{-1}$,[44] the equatorial (r_0) and axial (z_0) radii of the focal volume were 0.29 and 1.3 μm, respectively (effective volume 0.2 fL). By assuming a three-dimensional Gaussian-distributed excitation intensity, the ACF curves were fitted as described by Clamme et al.[44]

Cell toxicity: BY-2 cells were grown under standard conditions[26] in 24-well plates. Increasing concentrations of MG or MG derivatives (0, 0.125, 0.25, 0.5, 1.0, 2.0, 4.0 μM) were added, and after six days of incubation, pictures were taken, then pixel intensities were measured by using ImageJ and used as a measure of cell accumulation.

Acknowledgements

The authors thank Dr. Ludovic Riechert for TP-FCS experiments and Dr. Julien Godet for assistance in K_d determination. This work was performed with support from the ANR (grant ANR-08-BLAN-0244–02).

Keywords: aptamers · fluorescent probes · malachite green · RNA visualization · two-photon absorption

[1] O. Shimomura, F. H. Johnson, Y. Saiga, *J. Cell. Comp. Physiol.* **1962**, *59*, 223 – 239.
[2] M. Schmid, T. H. Jensen, *Chromosoma* **2008**, *117*, 419 – 429.
[3] P. Vinciguerra, F. Stutz, *Curr. Opin. Cell Biol.* **2004**, *16*, 285 – 292.
[4] S. L. Erickson, J. Lykke-Andersen, *J. Cell Sci.* **2011**, *124*, 293 – 297.
[5] K. Nagai, C. Oubridge, A. Kuglstatter, E. Menichelli, C. Isel, L. Jovine, *EMBO J.* **2003**, *22*, 3479 – 3485.
[6] D. St. Johnston, *Nat. Rev. Mol. Cell Biol.* **2005**, *6*, 363 – 375.
[7] B. Pyhtila, T. Zheng, P. J. Lager, J. D. Keene, M. C. Reedy, C. V. Nicchitta, *RNA* **2008**, *14*, 445 – 453.
[8] F. Besse, A. Ephrussi, *Nat. Rev. Mol. Cell Biol.* **2008**, *9*, 971 – 980.
[9] A. Eulalio, I. Behm-Ansmant, E. Izaurralde, *Nat. Rev. Mol. Cell Biol.* **2007**, *8*, 9 – 22.
[10] J. Xu, N.-H. Chua, *Curr. Opin. Plant Biol.* **2011**, *14*, 88 – 93.
[11] M. Ghildiyal, P. D. Zamore, *Nat. Rev. Genet.* **2009**, *10*, 94 – 108.
[12] D. H. Chitwood, M. C. Timmermans, *Nature* **2010**, *467*, 415 – 419.
[13] M. Heinlein, B. L. Epel, *Int. Rev. Cytol.* **2004**, *235*, 93 – 164.
[14] N. Christensen, J. Tilsner, K. Bell, P. Hammann, R. Parton, C. Lacomme, K. Oparka, *Traffic* **2009**, *10*, 536 – 551.
[15] S. Tyagi, F. R. Kramer, *Nat. Biotechnol.* **1996**, *14*, 303 – 308.
[16] E. Bertrand, P. Chartrand, M. Schaefer, S. M. Shenoy, R. H. Singer, R. M. Long, *Mol. Cell* **1998**, *2*, 437 – 445.
[17] J. Chen, O. Nikolaitchik, J. Singh, A. Wright, C. E. Bencsics, J. M. Coffin, N. Ni, S. Lockett, V. K. Pathak, W.-S. Hu, *Proc. Natl. Acad. Sci. USA* **2009**, *106*, 13535 – 13540.
[18] N. Daigle, J. Ellenberg, *Nat. Methods* **2007**, *4*, 633 – 636.
[19] T. Ozawa, Y. Natori, M. Sato, Y. Umezawa, *Nat. Methods* **2007**, *4*, 413 – 419.
[20] J. S. Paige, K. Y. Wu, S. R. Jaffrey, *Science* **2011**, *333*, 642 – 646.
[21] D. Grate, C. Wilson, *Proc. Natl. Acad. Sci. USA* **1999**, *96*, 6131 – 6136.
[22] J. R. Babendure, S. R. Adams, R. Y. Tsien, *J. Am. Chem. Soc.* **2003**, *125*, 14716 – 14717.
[23] D. F. Duxbury, *Chem. Rev.* **1993**, *93*, 381 – 433.
[24] R. Y. Tsien, *FEBS Lett.* **2005**, *579*, 927 – 932.
[25] M. Pawlicki, H. A. Collins, R. G. Denning, H. L. Anderson, *Angew. Chem.* **2009**, *121*, 3292 – 3316; *Angew. Chem. Int. Ed.* **2009**, *48*, 3244 – 3266.
[26] T. Surrey, M. B. Elowitz, P. E. Wolf, F. Yang, F. Nédélec, K. Shokat, S. Leibler, *Proc. Natl. Acad. Sci. USA* **1998**, *95*, 4293 – 4298.
[27] S. J. Remington, *Curr. Opin. Struct. Biol.* **2006**, *16*, 714 – 721.
[28] C. Baugh, D. Grate, C. Wilson, *J. Mol. Biol.* **2000**, *301*, 117 – 128.
[29] D. H. Nguyen, T. Dieckmann, M. E. Colvin, W. H. Fink, *J. Phys. Chem. B* **2004**, *108*, 1279 – 1286.
[30] D. H. Nguyen, S. C. DeFina, W. H. Fink, T. Dieckmann, *J. Am. Chem. Soc.* **2002**, *124*, 15081 – 15084.
[31] L. T. Nguyen, P. H. S. Kwakman, D. I. Chan, Z. Liu, L. de Boer, S. A. J. Zaat, H. J. Vogel, *Antimicrob. Agents Chemother.* **2011**, *55*, 2074 – 2083.
[32] T. Dieckmann, E. Suzuki, G. K. Nakamura, J. Feigon, *RNA* **1996**, *2*, 628 – 640.
[33] J. Flinders, S. C. DeFina, D. M. Brackett, C. Baugh, C. Wilson, T. Dieckmann, *ChemBioChem* **2004**, *5*, 62 – 72.
[34] D. J. Patel, A. K. Suri, F. Jiang, L. Jiang, P. Fan, R. A. Kumar, S. Nonin, *J. Mol. Biol.* **1997**, *272*, 645 – 664.
[35] D. M. Brackett, T. Dieckmann, *ChemBioChem* **2006**, *7*, 839 – 843.
[36] M. Albota, D. Beljonne, J.-L. Brédas, J. E. Ehrlich, J.-Y. Fu, A. A. Heikal, S. E. Hess, T. Kogej, M. D. Levin, S. R. Marder, D. McCord-Maughon, J. W. Perry, H. Röckel, M. Rumi, G. Subramaniam, W. W. Webb, X.-L. Wu, C. Xu, *Science* **1998**, *281*, 1653 – 1656.
[37] G. A. Kraus, I. Jeon, M. Nilsen-Hamilton, A. M. Awad, J. Banerjee, B. Parvin, *Molecules* **2008**, *13*, 986 – 994.
[38] S. J. Culp, P. W. Mellick, R. W. Trotter, K. J. Greenlees, R. L. Kodell, F. A. Beland, *Food Chem. Toxicol.* **2006**, *44*, 1204 – 1212.
[39] R. A. Mittelstaedt, N. Mei, P. J. Webb, J. G. Shaddock, V. N. Dobrovolsky, L. J. McGarrity, S. M. Morris, T. Chen, F. A. Beland, K. J. Greenlees, R. H. Heflich, *Mutat. Res.* **2004**, *561*, 127 – 138.
[40] T. Zahn, T. Braunbeck, *Toxicol. In Vitro* **1995**, *9*, 729 – 741.
[41] M. V. Bianco, F. C. Blanco, B. Imperiale, M. A. Forrellad, R. V. Rocha, L. I. Klepp, A. A. Cataldi, N. Morcillo, F. Bigi, *BMC Infect. Dis.* **2011**, *11*, 195 – 204.
[42] Y.-H. Kim, C. Lee, H. Go, K. Konishi, K. Lee, P. C. K. Lau, M.-H. Yu, *Arch. Biochem. Biophys.* **2010**, *494*, 159 – 165.
[43] T. Nagata, Y. Nemoto, S. Hasezawa, *Intl. Rev. Cytol.* **1992**, *132*, 1 – 30.
[44] J. P. Clamme, J. Azoulay, Y. Mély, *Biophys. J.* **2003**, *84*, 1960 – 1968.

Received: November 26, 2011
Published online on ■■ ■■, 0000

A library of malachite green derivatives was designed in order to improve two-photon detection of a malachite green RNA aptamer. Some of the prepared derivatives show remarkable affinity for the aptamer and improved two-photon brightness as measured by two-photon fluorescence correlation spectroscopy. These new derivatives show lower toxicity than the classical malachite green oxalate.

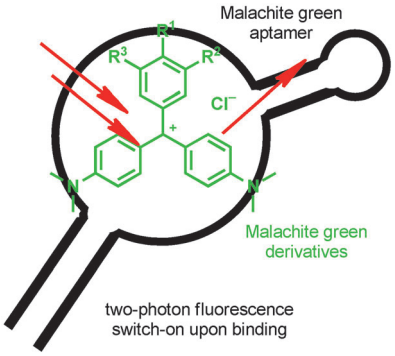

*J. Lux, E. J. Peña, F. Bolze, M. Heinlein, J.-F. Nicoud**

■■ – ■■

Malachite Green Derivatives for Two-Photon RNA Detection

